

Charged molecular silica trigger *in vitro* NETosis in human granulocytes via both oxidative and autophagic pathways

M. RIZZI¹, F. CARNIATO², S. TONELLO¹, M. MIGLIARIO¹, M. INVERNIZZI¹, V. ROCCHETTI¹, L. MARCHESE², F. RENÒ¹

¹Health Sciences Department, Università del Piemonte Orientale "A. Avogadro", Novara, Italy

²Dipartimento di Scienze e Innovazione Tecnologica and Nano-SiSTeMI Interdisciplinary Centre, Università del Piemonte Orientale "A. Avogadro", Alessandria, Italy

Abstract. – OBJECTIVE: Neutrophils play a key role in immunity and are known to respond to exogenous threats by releasing neutrophil extracellular traps (NETs) through NETosis, a process involving the release of neutrophils nuclear DNA decorated with proteins into the extracellular space.

In this study, attention has been focused on the ability of differently charged molecular systems polyhedral oligomeric silsesquioxanes (POSS) to induce NETosis.

MATERIALS AND METHODS: NETs formation was induced by phorbol myristate acetate (PMA) (positive control) and POSS treatment and visualized by confocal microscopy. Moreover, NETs production was quantified by Sytox green staining. Oxidative stress, autophagy as well as endocytosis involvement in the observed phenomena was evaluated by a specific inhibitory approach.

RESULTS: Results obtained in this study demonstrate a POSS time and dose-dependent ability in inducing NETs release irrespectively to their charge. POSS induced NETosis is a consequence of their internalization, as demonstrated by the strong reduction in NETs formation after endocytosis inhibition. Moreover, POSS induced NETosis involves both an increase in superoxide anion generation and autophagy pathway activation as demonstrated by the protective effect displayed by sodium azide and wortmannin.

CONCLUSIONS: Data presented in this study indicate that nanomaterials and molecular systems could have a role in the onset of inflammatory phenomena.

Key Words:

Autophagy, Granulocytes, NETs, Oxidative stress, POSS.

Introduction

Granulocytes play a pivotal role in the innate immune response. Pathogen invasion activates

neutrophils, a subclass of granulocytes, inducing the production of neutrophil extracellular traps (NETs) through a mechanism defined NETosis¹⁻³.

In recent years NETs formation has been widely investigated. *In vitro* experiments demonstrated that neutrophils activation resulting in NETs formation induces nuclear and granular membrane dissolution, leading to nuclear content decondensation into the cytoplasm. Then, plasma membrane rupture results in the release of the neutrophil nuclear content into the extracellular space. The NET scaffold is therefore composed of decondensed chromatin fibers with a 15-17 nm diameter, decorated with DNA and granular, as well as cytoplasmic proteins⁴⁻⁶.

NETs formation is a very quick process, occurring in only few minutes when induced by bacterial lipopolysaccharide-stimulated platelets under conditions of flow or few hours when induced by phorbol myristate acetate (PMA), *Staphylococcus aureus* or *Candida albicans* stimulation^{3,4,7}. Even if the molecular mechanisms underlying NETs formation are still not fully elucidated, there is evidence suggesting both reactive oxygen species (ROS) and autophagy involvement. Neutrophils' activation is known to be closely related to ROS production as such highly reactive molecules act as signaling molecules able to direct granulocyte physiology, thus playing a key role in the first step of NETs formation^{1,4,6,8}. Moreover, it has been observed that PMA-induced NETs formation is associated with autophagy induction and that such event is strictly dependent on the concomitant increase in the superoxide anion generation⁹.

In addition to be induced by pathogen invasion, NETs formation could be also induced by nanoparticles (NPs), as such compound are known to trigger granulocyte activation^{10,11}.

NPs are widely used as a model platform to prepare hybrid organic/inorganic materials of great interest for drug and gene delivery, biosensing and bioimaging applications¹². NPs in the bloodstream quickly activate monocytes and neutrophils based on their physical-chemical characteristics. In fact, it is well known that NPs shape and size, along with their charge, are important players in determining their interaction with the cell surface and intracellular fate after endocytosis¹³⁻¹⁵.

In the last years, polyhedral oligomeric silsesquioxanes (POSS) emerged as promising materials for different biomedical applications^{12,16-21}.

POSS are fascinating nanodimensional, easily synthesizable molecular compounds²²⁻²⁴. Their well defined structure is composed by an inorganic cage of silicon and oxygen atoms and by organic functionalities with tunable reactivity, attached to the apexes of the silica core. Typically, POSS molecules exhibited high thermal stability, outstanding chemical versatility and good compatibility with hydrophilic and hydrophobic environments.

Despite their emerging role as promising biomedical tools, to the best of our knowledge, extensive studies on POSS toxicity and interactions with cells was marginally investigated.

On the light of these considerations, the aim of this study was to investigate the effect of POSS bearing in their structure either positive groups (octa-ammonium POSS, POSS-NH₃⁺) or negative functionalities (octa-maleamate POSS, POSS-COO⁻) (Figure 1) in inducing human neutrophil activation and NETs release.

Materials and Methods

POSS-NH₃⁺ Synthesis

The octa-ammonium POSS (POSS-NH₃⁺) was synthesized by using Gravel and coworkers [25] synthetic procedure. Briefly, 20 mL of aminopropyl triethoxysilane were dissolved in 160 mL of methanol containing 27 mL of hydrochloric acid (37 wt%). The solution was maintained at 298 K under stirring for ten days. The reaction carried out for a long time promoted the formation of a white product that was separated and dried in an oven at 323 K for few hours.

POSS-COO⁻ Preparation

The carboxylate POSS (POSS-COO⁻) was obtained by deprotonation of the commercial octa-maleamic acid POSS (Hybrid Plastics Company). In detail, 1 g of octa-maleamic acid POSS was dispersed in 10 mL of water. The solution was corrected to pH 9.0 by adding drop-by-drop 1M sodium hydroxide solution. The suspension was stirred at 298 K for 1 h in order to promote the complete deprotonation of carboxylic arms linked to the POSS cage.

POSS Characterization Techniques

¹H and ²⁹Si NMR spectra were obtained by dissolving the samples in 600 μL of deuterated dimethylsulphoxide (0.1 M POSS). The analyses were carried out at 300 K by using a Jeol Eclipse Plus spectrometer equipped with an 8 T magnet.

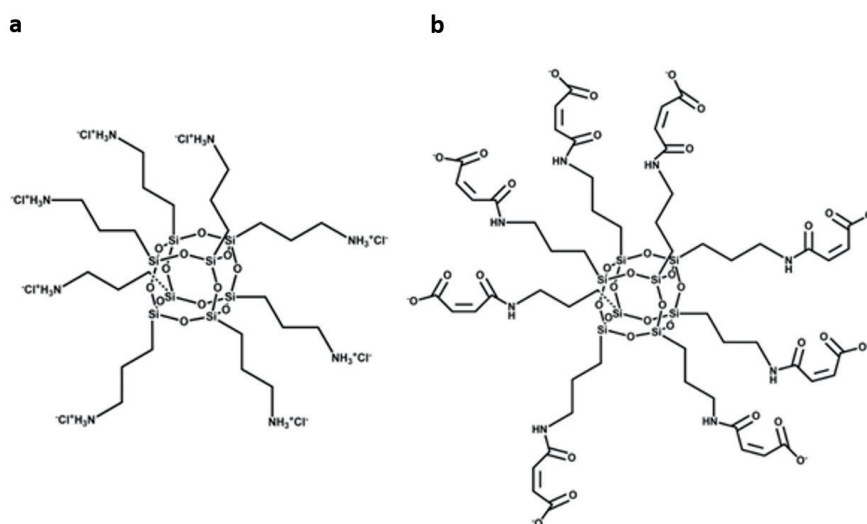


Figure 1. POSS structure. Chemical structure of POSS-NH₃⁺ (a) and POSS-COO⁻ (b).

Infrared spectra were collected with Bruker Equinox 55 spectrometer with resolution of 4 cm⁻¹ and in the range 4000-400 cm⁻¹. The samples were dispersed in potassium bromide matrix (10 wt%).

Zeta potential (ξ -potential) analyses were performed on POSS water solution with a Zetasizer NanoZS (Malvern,UK), equipped with a laser He-Ne ($\lambda_{em} = 633$ nm) working in a particle size range of 0.6 nm-6 μ m.

Plasma and Granulocytes Separation

Human peripheral venous blood (40 ml) was obtained from 5 healthy donors (30-40 years) using Lithium/Heparin (Vacutainer, Becton Dickinson, Franklin Lakes, NJ, USA) as anticoagulant. Blood specimen to isolate granulocyte fraction have been obtained after informed consent by healthy donors which blood have been collected for routine hematologic tests. Therefore, the entire procedure has been considered exempt from the need to obtain the Ethical Committee approval.

Blood was diluted 1:1 with phosphate buffer (PBS, pH=7.4) and separated onto Lympholyte-H (Cedarline, Burlington, Canada) cell separation medium. Erythrocytes were lysed using ammonium chloride lysis solution in ice. Isolated granulocytes were washed in sterile PBS, counted and suspended at a concentration of 1×10^6 cells/ml in RPMI 1640 medium supplemented with 10% heat inactivated fetal bovine serum (FBS) (Carlo Erba Reagents srl, Cornaredo, Italy).

Granulocytes Incubation with POSS

POSS aqueous solutions were prepared dissolving POSS-NH₃⁺ and POSS-COO⁻ in PBS. Granulocytes were incubated in the presence or absence of different amounts of POSS (0.05-1 mg/ml) for 240 min in a humidified atmosphere containing 5% CO₂ at 310 K 25. As positive control some samples were incubated, in the same conditions, with 100 nM PMA (Sigma Aldrich, St. Louis, MO, USA).

To evaluate NETs production kinetics, in some experiments granulocytes were incubated with PMA (100 nM) or POSS (1 mg/ml) for different times (5, 15, 30, 60, 120, 180, 240 min).

Inhibition Studies

To test the effect of clathrin vesicles and macropinocytosis inhibition, cells were incubated for 30 min with chlorpromazine (40 μ M) or amiloride (1 mM) before POSS stimulation²⁶.

The role of ROS generation and autophagy in NETosis was evaluated by pre-incubating granulocytes for 30 min with sodium azide (NaN₃, 1 mM) or wortmannin (WRT, 10 μ g/ml) (Sigma-Aldrich, St. Louis, MO, USA) respectively⁹.

NETs Quantification

NETs were quantified according to Vong and coworkers' protocol²⁶. Briefly 1×10^5 cells/well were seeded in HBSS buffer and stimulated with PMA 100 nM (to activate NETs formation), Triton X-100 (to evaluate total DNA content) or left untreated (control and DNase digested samples). After 2 hours 5U DNase were added to all the wells (excluding controls and Triton X-100 treated samples). 45 min after DNase addition, Sytox Green dye (Thermo Fisher Scientific, Waltham, MA, USA) was added to each well and the plate was incubated for further 15 min. Fluorescence ($\lambda_{ex}504$ nm/ $\lambda_{em}523$ nm) was then quantified using a microplate reader (Victor X4, Perkin Elmer, Waltham, MA, USA). Extracellular DNA content was expressed as percentage of total DNA obtained by subtracting the fluorescence intensity of the DNase containing wells from the comparative control and dividing the obtained result by the fluorescence intensity of Triton X-100 containing wells.

NETs Confocal Microscopy Visualization

For confocal microscopy visualization 5×10^3 cells were seeded on poly-lysine coated microscope slides and treated with POSS (0.05-1 mg/ml) in the presence or absence of amiloride (1 mM) chlorpromazine (40 μ M) sodium azide (1 mM) and wortmannin (10 μ g/ml) as previously described.

At the end of the experiments, cells were fixed overnight at 277 K in the dark using a 3.7% formaldehyde, 3% sucrose solution in PBS and observed using a Leica DMIRE2 confocal microscope (Leica, Wetzlar, Germany) operating in fluorescence with an Ar/HeNe laser (488 nm).

Statistical Analysis

Each experiment was performed in triplicate to assure statistical significance. One-way ANOVA followed by Bonferroni's post-hoc tests were done for statistical analysis. Statistical procedures were performed with the Prism 4.0 statistical software (GraphPad Software Inc., La Jolla, CA, USA). Probability values of $p < 0.05$ were considered statistically significant.

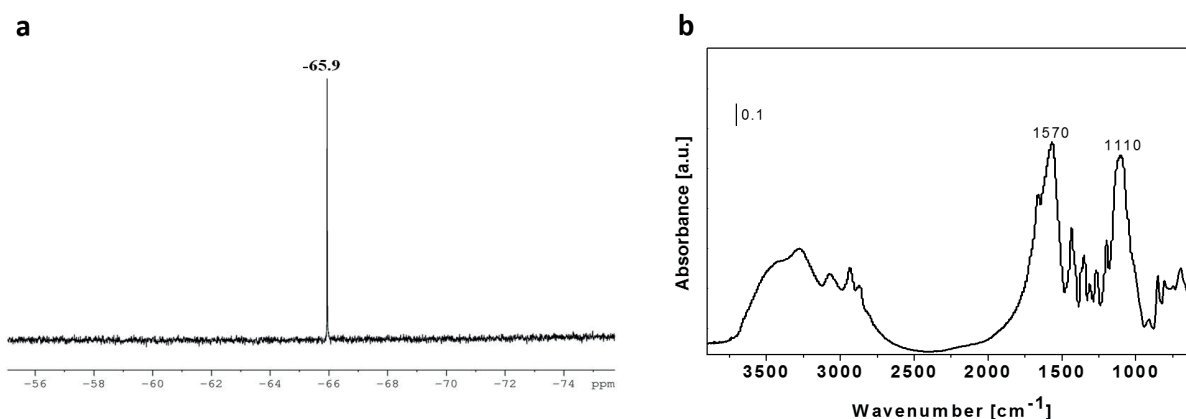


Figure 2. POSS chemical characterization. *A)* ^{29}Si NMR spectrum collected in deuterated dimethylsulphoxide of POSS-NH₃⁺. *B)* FT-IR spectrum of POSS-COO⁻ diluted in potassium bromide matrix. The analysis was performed at room temperature, in air.

Results

Two condensed polyhedral oligomeric silsesquioxanes, functionalized with positive ammonium groups (POSS-NH₃⁺) and negative carboxylate units (POSS-COO⁻) were selected for this study (Figure 1).

The first one was synthesized by adopting a procedure reported in the literature [24] [25]. The quality of the sample was monitored by NMR spectroscopy applied to ^1H and ^{29}Si nuclei. ^1H NMR spectrum collected in deuterated dimethylsulphoxide, showed different peaks at 0.72 (SiCH₂), 1.72 (SiCH₂CH₂CH₂NH₃⁺), 2.77 (SiCH₂CH₂CH₂NH₃⁺) and 8.27 ppm (SiCH₂CH₂CH₂NH₃⁺), assigned to the protons of methylene and -NH₃⁺ groups of the ammonium-propyl bound to POSS cage. ^{29}Si NMR spectrum is particularly indicative of the purity of the product. In fact, the spectrum was characterized by one defined peak at -65.9 ppm, attributed to the eight equivalent silicon nuclei composing the POSS cage (Figure 2A).

The charge density of POSS-NH₃⁺ was estimated in water, by dissolving 10 mg of the sample in 1 mL of pure water. This parameter was determined by Zeta potential (ζ -potential) analysis. The solution showed a very positive ζ -potential of +15 mV, promoted by the presence of -NH₃⁺ groups bound to the POSS cage.

The deprotonation of the carboxylic groups of the commercial octa-maleamic acid POSS was monitored by infrared spectroscopy. IR spectrum collected at room temperature and under air conditions for the sample diluted in potassium bromide (Figure 2B) showed along with the absorptions

typical of the siloxane cage (i.e. the peak at 1110 cm⁻¹ is attributed to the stretching mode of the Si-O-Si bonds and the bands in the 3070-2860 cm⁻¹ range are assigned to the stretching modes of the C-H groups) a very strong absorption at 1570 cm⁻¹ which can be attributed to the stretching modes of the COO⁻ moieties.

Furthermore, a confirmation of the POSS deprotonation is provided by the Zeta potential (ζ -potential) analysis. The POSS-COO⁻ charge density, estimated in water (10 mg of sample in 1 mL of water) was of -40 mV.

Effect of POSS Stimulation on NETs Formation

NETosis is the result of a strong granulocyte activation. As shown in Figure 3, granulocyte stimulation with PMA, a potent tumor promoter, results in a great increase in extracellular DNA content (27.9% ± 1.14%). In order to evaluate if POSS were able to activate granulocyte NETosis, cells were stimulated with growing concentrations of both positively and negatively charged POSS. Figure 3 shows that both POSS molecules were able to induce extracellular DNA production, even if with a lower efficiency compared to PMA. POSS induced NET formation was dose-dependent, irrespectively of their charge. Interestingly, NET quantification showed that low concentrations (0.05-0.5 mg/ml) of negatively charged POSS were able to induce a stronger granulocyte activation compared to positively charged POSS. Such charge dependent effect disappeared when cells were stimulated with the higher POSS concentration (1 mg/ml), finally resulting in an extracellular DNA content of 12.6% ± 2.98% and 16.48%

$\pm 2.15\%$ after positively and negatively charged POSS stimulation respectively.

The different ability of the two differently charged POSS in inducing NETs formation was confirmed also by confocal microscopy analysis (Figure 3B). Fluorescence images, in fact, showed a greater increase in NET formation after negatively charged POSS stimulation.

In order to better elucidate the mechanism underlying POSS induced NET formation, kinetics studies were performed by stimulating human granulocytes with POSS concentration resulting

in the higher extracellular DNA production (1 mg/ml).

Figure 4 shows a time-dependent increase in NET production after each stimulation. PMA induced extracellular DNA production reached a plateau value starting from 60 min stimulation. Negatively charged POSS induced extracellular DNA production grew with time until reaching a plateau value starting from 120 min stimulation. On the other hand, positively charged POSS showed a different kinetic profile, inducing an extracellular DNA accumulation increasing linearly with time.

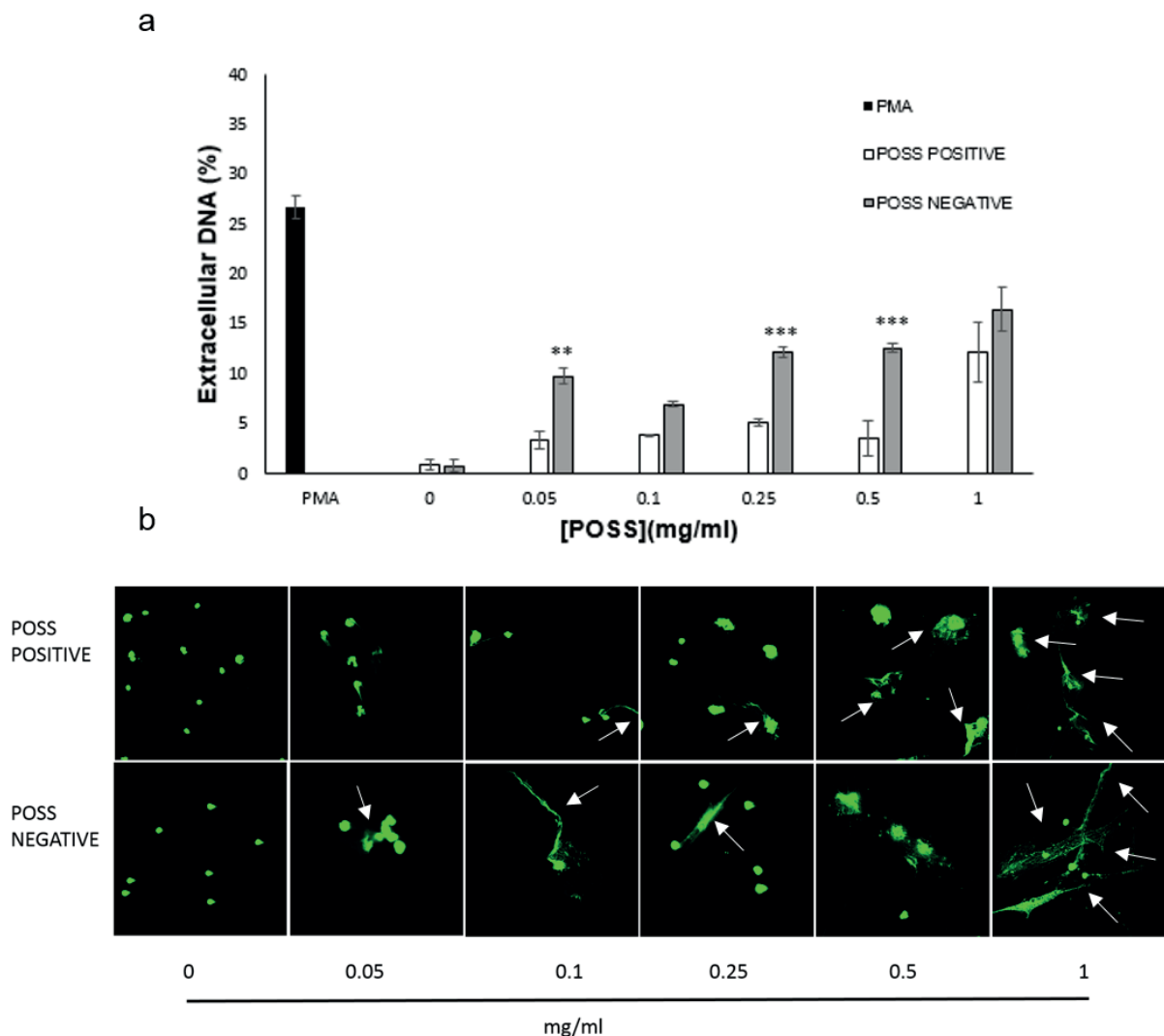


Figure 3. POSS induced NETs formation. Granulocytes were stimulated with increasing POSS concentrations for 240 min and fixed in 3.7% formaldehyde, 3% sucrose solution in PBS before DNA staining with sytox green dye. **A)** Extracellular DNA quantification. PMA 100 nM (black bar) represents the positive control. White bars represent positively charged POSS while gray bars represent negatively charged POSS. ** $p < 0.01$, *** $p < 0.001$ positively charged POSS vs. negatively charged POSS. **B)** Representative confocal images of POSS induced NET production. White arrows indicate NETs (40 X).

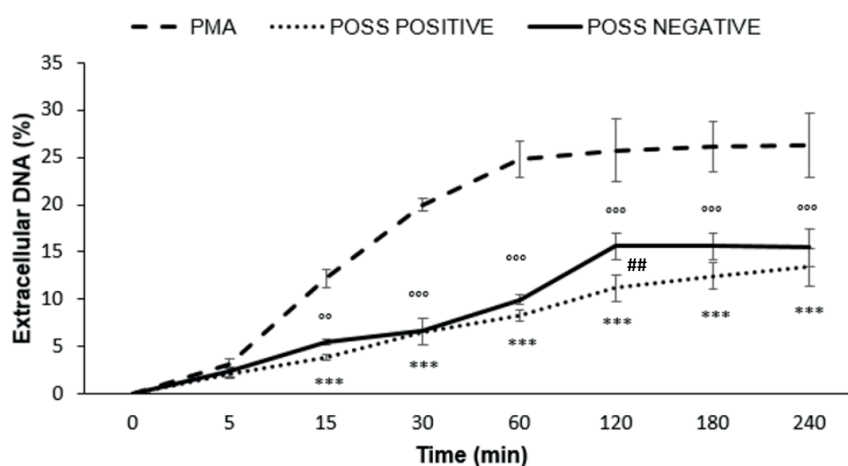


Figure 4. POSS induced NETs formation kinetics. PMA 100 nM (dashed line) represents the positive control. POSS were tested at 1 mg/ml concentration. Dotted line represents positively charged POSS while full line represents negatively charged POSS. *** $p < 0.001$ positively charged POSS vs. PMA; °°° $p < 0.01$, °°° $p < 0.001$ negatively charged POSS vs. PMA; ## $p < 0.01$ POSS positive vs. POSS negative.

Inhibition Studies

It has been supposed that POSS induced NETosis depends on their internalization: for this reason, endocytosis inhibition studies were performed using chlorpromazine and amiloride as blocking agents. In particular, chlorpromazine was used to inhibit clathrin vesicle-mediated internalization while amiloride was used to inhibit macropinocytosis. As shown in Figure 5, granulocyte pre-treatment with the inhibitors strongly decreased extracellular DNA accumulation. In control conditions (cells without pre-treatment), NET production pattern was similar to that described in Figure 3. When the clathrin vesicle production was inhibited by chlorpromazine pre-treatment, POSS induced NET production was strongly reduced. Moreover, also macropinocytosis inhibition by amiloride showed a similar effect. Interestingly, endocytosis inhibition resulted in a strong reduction of extracellular DNA content independently of POSS chemical nature (Figure 5A, B).

The observed reduction in POSS induced NET formation after endocytosis inhibition was confirmed also by morphological evaluation on confocal microscopy images (Figure 5C).

In addition to POSS endocytosis involvement in NETosis, a key role for autophagy and oxidative stress was also speculated. In order to verify such hypothesis, cells were incubated with wortmannin (an autophagy pathway inhibitor) or sodium azide (a superoxide anion scavenger) before POSS stimulation.

As shown in Figure 6, PMA and POSS alone showed an extracellular DNA accumulation profile similar to that observed in Figure 3. Autophagy inhibition by wortmannin resulted in a strong reduction in NET production after positively or negatively charged POSS stimulation. NETs formation was strongly reduced also after sodium azide pre-treatment, irrespectively of POSS charge (Figure 6A, B).

Such reduction in POSS induced NET formation was confirmed also by morphological evaluation on confocal microscopy images (Figure 6 C, D).

Discussion

Human immune system is composed of a complex network of cells and molecules whose main function is to protect the organism from invading pathogens and noxious compounds. For long time, neutrophils have been considered only a downstream player of immune response, mainly acting through phagocytosis and release of antimicrobial agents by degranulation^{3,8}. In the last decade, growing evidence revealed also a third neutrophils' mode of action, represented by NETs formation^{3,4,6}.

NET antimicrobial activity is mediated by their ability to provide high local concentration of antimicrobial molecules effectively killing invading pathogens. Moreover, they play a pivotal role in protecting the organism from invading agents too large to be effectively phagocytosed⁶.

Another interesting hallmark of NET is represented by their ability to act as signaling com-

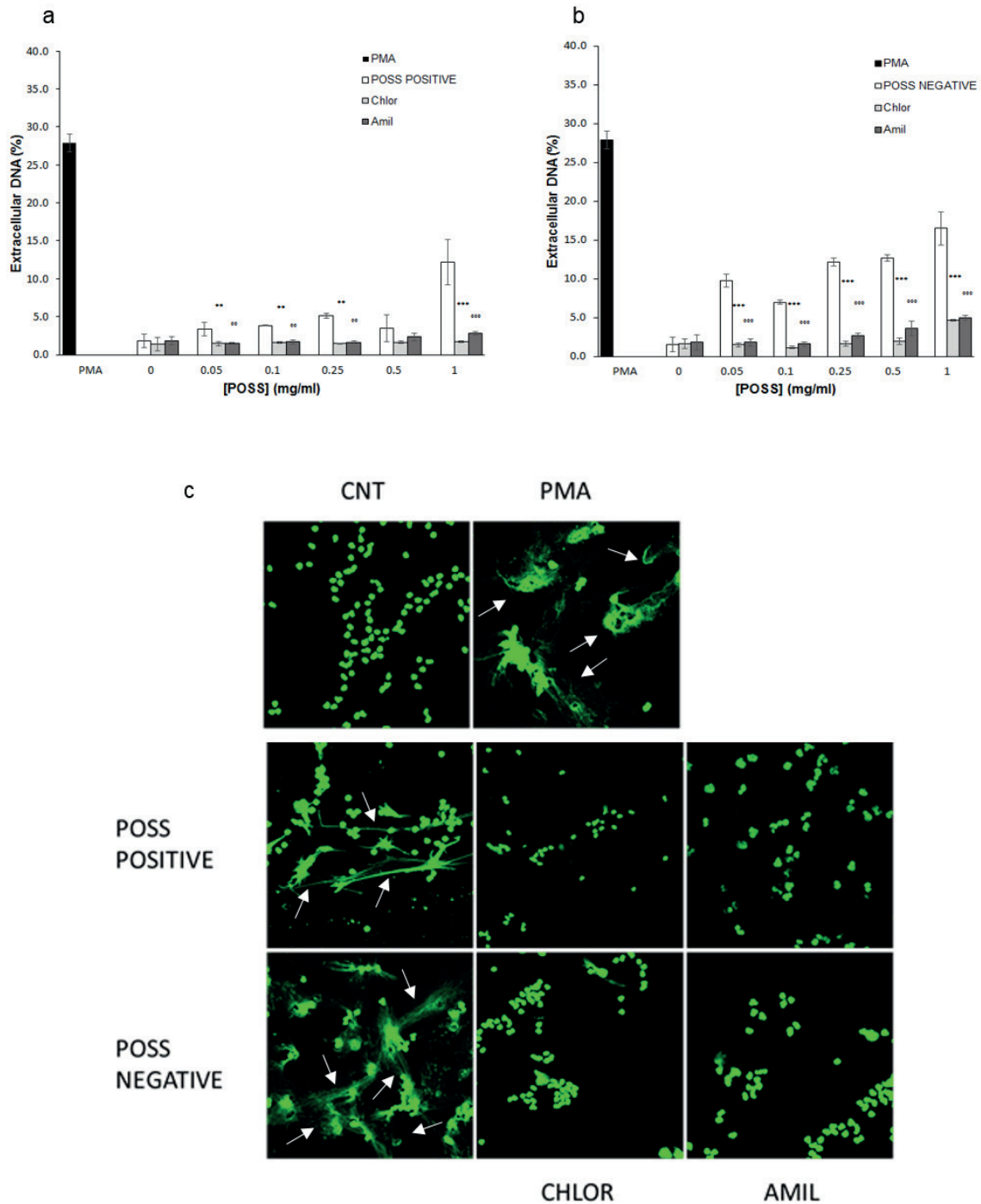


Figure 5. POSS induced NETs formation inhibition by uptake inhibitors. Granulocytes were stimulated with increasing POSS concentrations for 240 min and fixed in 3.7% formaldehyde, 3% sucrose solution in PBS before DNA staining with sytox green dye. Extracellular DNA production was quantified after positively (a) and negatively (b) charged POSS treatment in the presence or absence of chlorpromazine (chlor, 40 μ M) and amiloride (amil, 1 mM). PMA 100 nM (black bar) represents the positive control. White bars represent positively (panel a) or negatively (panel b) charged POSS. Light gray bars represent chlorpromazine pre-treatment while dark gray bars represent amiloride pre-treatment. ** $p < 0.01$, *** $p < 0.001$ chlorpromazine referred to POSS alone; °° $p < 0.01$, °°° $p < 0.001$ amiloride referred to POSS alone. c) Representative confocal images of POSS (1 mg/ml) induced NET production in the presence or absence of chlorpromazine and amiloride. White arrows indicate NETs (40 X).

pounds modulating inflammatory responses, as they are very abundant at inflammatory sites, as observed in human appendicitis and in an experimental model of shigellosis^{3,6}.

Although the first experimental evidence placed NET formation within the context of innate immune response to infections, growing evidence suggests a strong involvement of these structures in the pathogenesis of several diseases, acting as a putative source of immune effectors and pro-inflammatory mediators⁴. Recently, NET release acquired a growing interest in autoimmunity⁴. The evidence that several molecules decorating

chromatin scaffold are recognized as autoantigens supports the hypothesized involvement of NET in autoimmune response in predisposed individuals. Moreover, it has been observed that autoimmune responses are initiated or exacerbated following microbial infections, condition triggering NET production^{4,6}. On the other hand, alterations in NET clearance machinery may also be associated with autoimmune disease onset^{6,28}. Even if NETs production is many often associated to a “bad” role, exacerbating inflammatory responses, in some circumstances they could also have a positive role, favoring inflammation

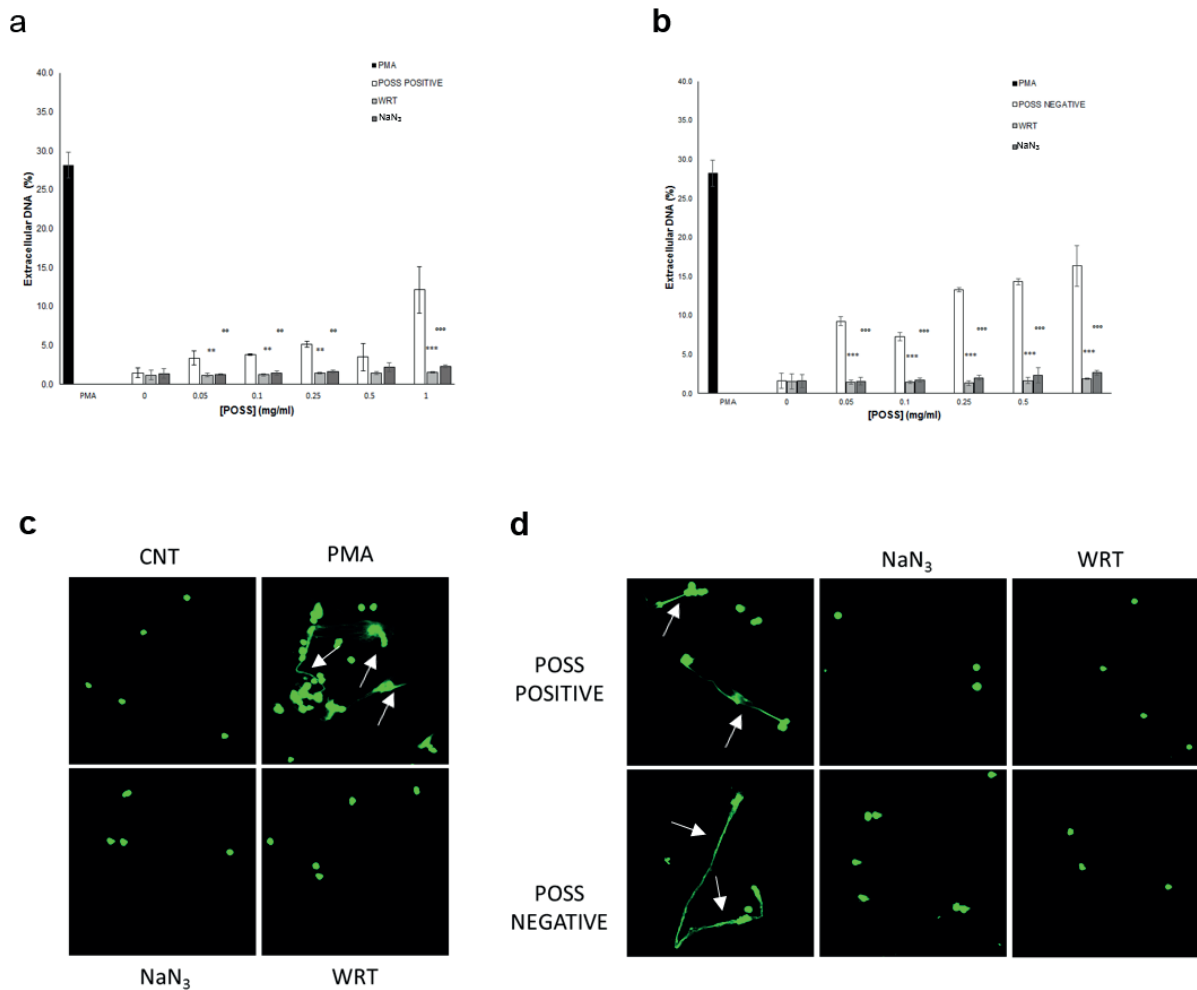


Figure 6. POSS induced NETs formation inhibition by azide and wortmannin. Granulocytes were stimulated with increasing POSS concentrations for 240 min and fixed in 3.7% formaldehyde, 3% sucrose solution in PBS before DNA staining with sytox green dye. Extracellular DNA production was quantified after positively (a) and negatively (b) charged POSS treatment in the presence or absence of sodium azide (NaN₃, 1 mM) and wortmannin (WRT, 10 μg/ml). PMA 100 nM (black bar) represents the positive control. White bars represent positively (panel a) or negatively (panel b) charged POSS. Light gray bars represent WRT pre-treatment while dark gray bars represent NaN₃ pre-treatment. ***p*<0.01, ****p*<0.001 wortmannin referred to POSS alone; °°*p*<0.01, °°°*p*<0.001 NaN₃ referred to POSS alone. c) Representative confocal images of PMA, NaN₃ and Wortmannin induced NET production. White bars indicate NETs (40 X). d) Representative confocal images of POSS induced NET formation in the presence or absence of NaN₃ and WRT. White arrows indicate NETs (40 X).

resolution, as demonstrated in the case of gouty arthritis, a pathological condition in which monosodium urate crystals are seen by circulating granulocytes as a potentially noxious compound and therefore entrapped in NETs network, in order to protect the surrounding tissues^{8,29}. Recent advances in nanotechnological field resulted in a great increase in human organism exposure to nanomaterials. By definition, nanomaterials dimensions are similar to that of physiological molecules such as proteins and nucleic acids and, for this reason, have been widely exploited for various biomedical applications. Material bulk properties change considerably at the nanoscale level, resulting in nanomaterials displaying superior mechanical, thermal, electrical, magnetic and optical properties of great interest in biomedicine. Among nanomaterials, particles with a diameter of less than 100 nm are called nanoparticles and represent a very interesting class of compounds^{10,20}.

It is well known that NPs rapidly activate immune response and that charged functionalities exposed on their surface directly affects their uptake mechanism. Moreover, NPs administration has been described to be able to specifically activate neutrophils, finally inducing NETs formation^{10,13,16}.

POSS are three-dimensional, cage-like nanostructures characterized by the possibility of easy chemical modification. Moreover, POSS derivatives have been shown to physically resist to a variety of thermal and chemical experimental conditions, thus suggesting a high *in vivo* stability along with good compatibility with hydrophilic as well as hydrophobic environments^{30,31}.

Due to their high water solubility, low cytotoxicity and high biocompatibility, POSS can be used to build novel nanocomposites for biomedical imaging, drug delivery and tissue engineering applications¹⁶⁻²¹, representing an interesting alternative to the multifunctional nanocarriers reported in the literature^{12,32,33}.

To the best of our knowledge, POSS possible toxicity and the role of charged functionalities on their surface in mediating POSS-cells interactions was marginally investigated.

Results presented in this paper show that human granulocyte stimulation with POSS, either positively or negatively charged, is able to induce NETs formation in a dose-dependent manner. As surface charged functionalities are known to deeply influence NPs/cell interactions, attention has been focused on POSS chemical nature, showing that negatively charged POSS induced a greater

release of extracellular DNA compared to positively charged ones.

In order to better understand the observed phenomenon, attention has also been focused on NET release kinetics. The different NETs formation inducing ability of differently charged POSS was reflected also in the extracellular DNA release kinetics.

POSS small size and high charge density facilitate their uptake by both tissues and cells³⁰. Uptake inhibition studies performed using chlorpromazine³⁴⁻³⁶ and amiloride³⁴ as endocytosis inhibitors showed a reduction in POSS induced NET release, thus suggesting a possible involvement of POSS internalization in initiating NETs formation. Both inhibitors reduced, quite at the same extent, POSS induced NET production, thus suggesting that there is not a preferred uptake mechanism for such molecular systems when inducing NETs formation.

Results also highlight that POSS not only induce NET release after internalization, but can also act through a different mechanism, by increasing superoxide anion generation and by activating autophagy pathway. ROS involvement in NETosis initiation has been confirmed by cells pre-treatment with sodium azide, a well-known superoxide anion scavenger, finally resulting in a strong reduction in extracellular DNA release. On the other hand, autophagy involvement has been confirmed by granulocytes pre-treatment with wortmannin, an autophagy blocker, resulting in a strong reduction in NET release. Wortmannin is a Phosphatidylinositol-4,5-bisphosphate 3-kinase (PI3K) inhibitor that rules the mTOR pathway and the autophagy process^{9,37,38}.

These data are in agreement with Remijsen et al⁹ results, showing that a combination of autophagy and superoxide production is necessary for PMA induced NETs formation.

Conclusions

Data presented in this study indicate a possible involvement of NPs and molecular systems in the onset of inflammatory phenomena as well as in its resolution, highlighting the necessity of an even increasing attention to their biomedical applications.

Funding

The study was supported by University local funds and by a Fondazione Comunità Novarese Onlus grant.

Acknowledgments

The authors gratefully thanks Prof. Umberto Dianzani (Immunology Lab, Università del Piemonte Orientale, Novara Italy) for the interesting scientific discussions.

Conflict of Interest

The Authors declare that they have no conflict of interest.

References

- BRINKMANN V, REICHARD U, GOOSMANN C, FAULER B, UHLEMANN Y, WEISS DS, WEINRAUCH Y, ZYCHLINSKY Y. Neutrophil extracellular traps kill bacteria. *Science* 2014; 303: 1532-1535.
- M'OCSEI A. Diverse novel functions of neutrophils in immunity, inflammation, and beyond. *J Experiment Med* 2010; 210: 1283-1299.
- FUCHS TA, ABED U, GOOSMANN C, HURWITZ R, SCHULZ I, WAHN V, WEINRAUCH Y, BRINKMANN V, ZYCHLINSKY A. Novel cell death program leads to neutrophil extracellular traps. *J Cell Biol* 2007; 176: 231-241.
- KAPLAN MJ, RADIC M. Neutrophil extracellular traps: double-edged swords of innate immunity. *J Immunol* 2012; 189: 2689-2695.
- YIPP BG, PETRI B, SALINA D, JENNE CN, SCOTT BN, ZBYTNUK LD, PITTMAN K, ASADUZZAMAN M, WU K, MEIJNDERT HC, MALAWISTA SE, DE BOISFLEURY CHEVANCE A, ZHANG K, COLNY J, KEBES P. Infection-induced NETosis is a dynamic process involving neutrophil multitasking in vivo. *Nat Med* 2012; 18: 1368-1393.
- PAPAYANNOPOULOS V, ZYCHLINSKY A. NETs: a new strategy for using old weapons. *Trends Immunol* 2009; 30: 513-521.
- LUAN SX, CHEN XH. Th glucocorticoids inhibit neutrophils formed extracellular traps (NETs) and suppress inflammation caused by fallopian tube staphylococcal infection. *Eur Rev Med Pharmacol Sci* 2017; 21: 855-860
- HAHN J, KNOPF J, MAUERÖDER C, KIENHÖFER D, LEPPKES M, HERRMANN M. Neutrophils and neutrophil extracellular traps orchestrate initiation and resolution of inflammation. *Clin Exp Rheumatol* 2016; 34: 6-8.
- REMIJSEN O, VANDEN BERGHE T, WIRABWAN E, ASSELBERGH B, PARTHOENS E, DE RYCKE R, NOPPEN S, DELFORGE M, WILLEMS J, VANDENABEELE P. Neutrophil extracellular trap cell death requires both autophagy and superoxide generation. *Cell Res* 2001; 21: 290-304
- MUÑOZ LE, BILLY R, BIERMANN MH, KIENHÖFER D, MAUERÖDER C, HAHN J, BRAUNER JM, WEIDNER D, CHEN J, SCHARIN-MEHLMANN M, JANKO C, FRIEDRICH RP, MIELENZ D, DUMYCH T, LOOTSIK MD, SCHAUER C, SCHETT G, HOFFMANN M, ZHAO Y, HERMANN M. Nanoparticles size-dependently initiate self-limiting NETosis-driven inflammation. *Proc Natl Acad Sci U S A* 2016; 113: E5856-E5865.
- LIZ R, SIMARD JC, LEONARDI LB, GIRARD D. Silver nanoparticles rapidly induce atypical human neutrophil cell death by a process involving inflammatory caspases and reactive oxygen species and induce neutrophil extracellular traps release upon cell adhesion. *Int Immunopharmacol* 2015; 28: 616-625.
- OLIVERO F, RENÒ F, CARNIATO F, RIZZI M, CANNAS M, MARCHESI L. A novel luminescent bifunctional POSS as a molecular platform for biomedical applications. *Dalton Trans* 2012; 41: 7467-7473.
- BARTNECK M, KEUL H, ZWADLO-KLARWASSER A, GROLL J. Phagocytosis independent extracellular nanoparticle clearance by human immune cells. *Nano Lett* 2010; 10: 59-63.
- VERMA A, STELLACCI F. Effect of surface properties on nanoparticle-cell interactions. *Small* 2010; 6: 12-21.
- NAM HY, KWON SM, CHUNG H, LEE SY, KWON SH, JEON H, KIM Y, PARK H, KIM J, HER S, OH YK, KWON IC, KIM K, JEONG SY. Cellular uptake mechanism and intracellular fate of hydrophobically modified glycol chitosan nanoparticles. *J Control Release* 2009; 135: 259-267.
- SHEN C, HAN Y, WANG B, TANG J, CHEN H, LIN Q. Ocular biocompatibility evaluation of POSS nanomaterials for biomedical material applications. *RSC Adv* 2015; 5: 53782-53788.
- SOLOUK A, COUSINS BG, MIRAHMADI F, MIRZADEH H, NADOUSHAN MRJ, SHOKRGOZAR MA. Biomimetic modified clinical-grade POSS-PCU nanocomposite polymer for bypass graft applications: A preliminary assessment of endothelial cell adhesion and haemocompatibility. *Mater Sci Eng C* 2015; 46: 400-408.
- HÖRNER S, FABRITZ S, HERCE HD, AVRUTINA O, DIETZ C, STARK RW. Cube-octameric silsesquioxane-mediated cargo peptide delivery into living cancer cells. *Org Biomol Chem* 2013; 11: 2258-2265.
- PÉREZ-OJEDA ME, TRASTOY B, ROL Á, CHIARA MD, GARCÍA-MORENO I, CHIARA JL. Controlled click-assembly of well-defined hetero-bifunctional cubic silsesquioxanes and their application in targeted bioimaging. *Chem Eur J* 2013; 19: 6630-6640.
- RIZVI SB, YILDIRIM L, GHADERI S, RAMESH B, SEIFALIAN AM, KESHITGAR M. A novel POSS-coated quantum dot for biological application. *Int J Nanomed* 2012; 7: 3915-3927.
- GHANBARI H, COUSINS BG, SEIFALIAN AM. A nanocage for nanomedicine: polyhedral oligomeric silsesquioxane (POSS). *Macromol Rapid Commun* 2011; 31: 1032-1046.
- PESCARMONA PP, MASCHMEYER T. Oligomeric silsesquioxanes: synthesis, characterization and selected applications. *Aust J Chem* 2001; 54: 583-596.
- HARRISON PG. Silicate cages: precursors to new materials. *J Organomet Chem* 1997; 542: 141-183.
- BANEY RH, SAKAKIBARA A, SUZUKI T. Silsesquioxanes. *Chem Rev* 1995; 95: 1409-1430.
- GRAVEL MC, ZHANG C, DINDERMAN M, LAINE RM. Octa(3-chloroammoniumpropyl) octasilsesquioxane. *Appl Organomet Chem* 1999; 13: 329-336.
- RENÒ F, CARNIATO F, RIZZI M, OLIVERO F, PITTARELLA P, MARCHESI L. Flow cytometry evidence of human granulocytes interaction with polyhedral oligome-

- ric silsesquioxanes: effect of nanoparticle charge. *Nanotechnol* 2013; 24: 185101.
- 27) VONG L, SHERMAN PM, GLOGAUER M. Quantification and visualization of neutrophil extracellular traps (NETs) from murine bone marrow-derived neutrophils. *Methods Mol Biol* 2013; 1031: 41-50.
- 28) ALLAM R, KUMAR SV, DARISIPUDI MN, ANDERS HJ. Extracellular histones in tissue injury and inflammation. *J Mol Med* 2014; 92: 465-472.
- 29) SIL P, CRAIG P, REAVES BJ, BREEN P, QUINN S, SOKOLOVE J, RADA B. P2Y6 receptor antagonist MRS2578 inhibits neutrophil activation and aggregated neutrophil extracellular trap formation induced by gout-associated monosodium urate crystals. *J Immunol* 2016; 198: 428-442.
- 30) RIZVI SB, YANG SY, GREEN M, KESHTGAR M, SEIFALIAN AM. Novel POSS-PCU nanocomposite material as a biocompatible coating for quantum dots. *Bioconjug Chem* 2015; 26: 2384-2396.
- 31) MCCUSKER C, CARROLL JB, ROTELLO VM. Cationic polyhedral oligomeric silsesquioxane (POSS) units as carriers for drug delivery processes. *Chem Commun* 2005; 28: 996-998.
- 32) GE X, DONG L, SUN L, SONG Z, WEI R, SHI L, CHEN H. New nanoplatforms based on UCNPs linking with polyhedral oligomeric silsesquioxane (POSS) for multimodal bioimaging. *Nanoscale* 2015; 7: 7206-7215.
- 33) AL-RASHEED NM, AL-RASHEED NM, ABDEL BAKY NA, FADDAH LM, FATANI AJ, HASAN IH, MOHAMAD RA. Prophylactic role of α -lipoic acid and vitamin E against zinc oxide nanoparticles induced metabolic and immune disorders in rat's liver. *Eur Rev Med Pharmacol Sci* 2014; 18: 1813-1828.
- 34) BANNUNAH AM, VLLASALIU D, LORD J, STOLNIK S. Mechanisms of nanoparticle internalization and transport across an intestinal epithelial cell model: effect of size and surface charge. *Mol Pharm* 2014; 11: 4363-4373.
- 35) HUANG HC, CHEN CC, CHANG WC, TAO MH, HUANG C. Entry of hepatitis B virus into immortalized human primay hepatocytes by clathrin-dependent endocytosis. *J Virol* 2012; 86: 9443-9453.
- 36) GÖTTE M, SOFEU HEUGAING DD, KRESSE H. Biglycan is internalized via chlorpromazine-sensitive route. *Cell Mol Biol Lett* 2004; 9: 475-481.
- 37) ESKELINEN EL. New insights into the mechanisms of macroautophagy in mammalian cells. *Int Rev Cell Mol Biol* 2008; 266: 207-247.
- 38) LEVINE B, KROEMER G. Autophagy in the pathogenesis of disease. *Cell* 2008; 132: 27-42.